Finite-energy f-sum rules for valence electrons

D. Y. Smith
Argonne National Laboratory, Argonne, Illinois 60439

E. Shiles
Argonne National Laboratory, Argonne, Illinois 60439
and Virginia Commonwealth University, Richmond, Virginia 23284

(Received 7 December 1977)

The number of electrons effective in optical processes up to an energy ω, $n_{\rm eff}(\omega)$, may be defined in three distinct ways, a situation which had led to considerable confusion. This is a consequence of the fact that oscillator-strength sums may be constructed from the imaginary part of the dielectric function $\epsilon_2(\omega)$, the extinction coefficient $\kappa(\omega)$, or the energy-loss function $\mathrm{Im}[\epsilon^{-1}(\omega)]$. Here these quantities are investigated for an electronic system embedded in a polarizable medium of dielectric constant ϵ_b. This model closely approximates valence electrons moving in the background of polarizable ion cores in a condensed phase. The oscillator-strength sums are found to differ significantly and are not simply related at energies for which the embedded system's oscillator strength is not exhausted. In the limit in which exhaustion occurs, the sums differ only because of the shielding effects of the polarizable medium. The f sum for $\epsilon_2(\omega)$ then yields the system's conventional oscillator strength while the f sums for $\kappa(\omega)$ and $\mathrm{Im}[\epsilon^{-1}(\omega)]$ yield effective "strengths" that are reduced from the conventional value by factors of $\epsilon_b^{-1/2}$ and ϵ_b^{-2}, respectively. Similar results hold for the three definitions of $n_{\rm eff}(\omega)$. The analysis of a system in terms of partial f sums is shown to provide a check on the self-consistency of optical data as well as a means of determining core polarizabilities. These effects are illustrated for metallic aluminum.

I. INTRODUCTION

The Thomas-Reiche-Kuhn f-sum rule[1] has proved to be one of the principal guides to the analysis of optical spectra.[2] The rule may be expressed in a number of equivalent forms,[3] but in all cases the exact result involves knowledge of a function describing dissipative processes over all frequencies.

In the present paper we consider a class of finite f sums for a system embedded in a medium with constant polarizability, a situation closely realized in condensed phases by valence electrons moving in the "medium" of the polarizable ion cores.[4] It is shown that partial f sums for the dielectric function, the extinction coefficient, and the energy-loss function differ because of the polarization of the inner core levels. The results are then employed to discuss the separation of valence-electron oscillator strength from the effects of core polarization. The application of partial f sums as a self-consistency check on optical data is demonstrated for metallic aluminum.

II. PARTIAL f SUMS AND $n_{\rm eff}(\omega)$

The f sum rule may be written in three formally distinct forms for the analysis of optical spectra. These involve the imaginary part of the dielectric function $\epsilon_2(\omega)$, the imaginary part of the refractive index $\kappa(\omega)$, and the energy-loss function $\mathrm{Im}[\epsilon^{-1}(\omega)]$. The three forms are[3]

$$\int_0^\infty \omega\epsilon_2(\omega)\,d\omega = \frac{\pi}{2}\omega_p^2\,, \tag{1}$$

$$\int_0^\infty \omega\kappa(\omega)\,d\omega = \frac{\pi}{4}\omega_p^2\,, \tag{2}$$

and

$$\int_0^\infty \omega\,\mathrm{Im}[\epsilon^{-1}(\omega)]\,d\omega = -\frac{\pi}{2}\omega_p^2\,, \tag{3}$$

where ω_p is the plasma frequency $[4\pi Ne^2/\mathrm{m}]^{1/2}$, N denoting the electron density. While formally distinct, these rules have a common basis in causality and the equations of motion.[5]

In analogy with these f-sum rules it has become common practice to define the effective number density of electrons contributing to the optical properties up to an energy ω by the partial f sums[2]

$$n_{\rm eff}(\omega)\big|_\epsilon = \frac{\mathrm{m}}{2\pi^2e^2}\int_0^\omega \omega'\epsilon_2(\omega')\,d\omega'\,, \tag{4}$$

$$n_{\rm eff}(\omega)\big|_\kappa = \frac{\mathrm{m}}{\pi^2e^2}\int_0^\omega \omega'\kappa(\omega')\,d\omega'\,, \tag{5}$$

and

$$n_{\rm eff}(\omega)\,\big|_{\epsilon^{-1}} = -\frac{\mathrm{m}}{2\pi^2e^2}\int_0^\omega \omega'\,\mathrm{Im}[\epsilon^{-1}(\omega')]\,d\omega'\,. \tag{6}$$

Here the subscripts ϵ, κ, and ϵ^{-1} are used to distinguish the partial f sums involving $\epsilon_2(\omega)$, $\kappa(\omega)$, and $\mathrm{Im}[\epsilon^{-1}(\omega)]$, respectively. For reference, examples of these partial f sums for a model insulator and a model metal in free space are given in

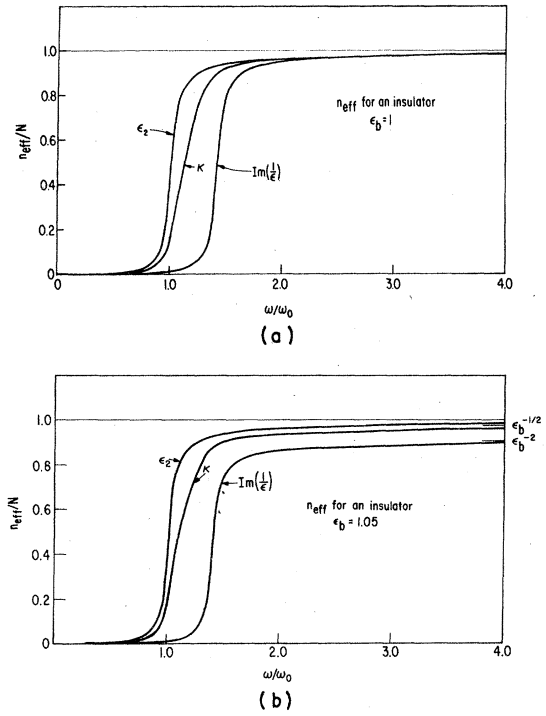

FIG. 1. Values of $n_{\mathrm{eff}}(\omega)$ for a single Lorentz oscillator model of an insulator (a) in free space (b) embedded in a dielectric medium with dielectric constant $\epsilon_b = 1.05$. Curves marked ϵ_2, κ, and $\mathrm{Im}(1/\epsilon)$ are for the integrands $\omega\epsilon_2(\omega)$, $\omega\kappa(\omega)$, and $\omega\,\mathrm{Im}[\epsilon^{-1}(\omega)]$, respectively. The Lorentz oscillator parameters used are $\omega_p = \omega_0$ and $\gamma = \frac{1}{10}\omega_0$ (for definitions see Ref. 6).

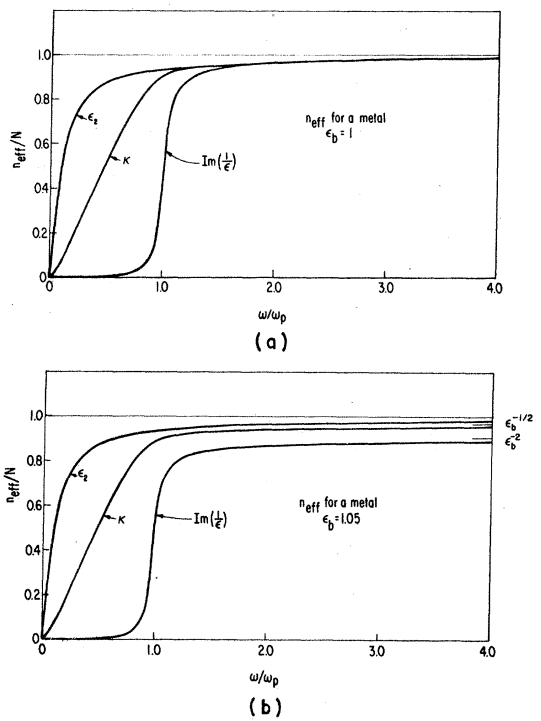

FIG. 2. Values of $n_{\mathrm{eff}}(\omega)$ for a Drude metal (a) in free space and (b) embedded in a dielectric medium with dielectric constant $\epsilon_b = 1.05$. The notation is the same as in Fig. 1 with parameters $\omega_0 = 0$ and $\gamma = \frac{1}{10}\omega_p$.

Figs. 1(a) and 2(a), respectively.

The reason for the difference in these definitions of $n_{\mathrm{eff}}(\omega)$ is that the integrands describe different properties of matter: $\epsilon_2(\omega)$ is a measure of the rate of energy dissipation from an electromagnetic wave, $\kappa(\omega)$ measures the decrease in amplitude of the wave, and $\mathrm{Im}[\epsilon^{-1}(\omega)]$ is related to the energy lost by a fast charged particle.

The differences may be explicitly demonstrated by writing the integrals in terms of common functions, say, the real and imaginary parts of the refractive index, $n(\omega)$ and $\kappa(\omega)$, respectively. This yields for Eqs. (4) and (6)

$$n_{\mathrm{eff}}(\omega)|_{\epsilon} = \frac{m}{\pi^2 e^2}\int_0^{\omega} \omega' n(\omega')\kappa(\omega')\,d\omega' \tag{7}$$

and

$$n_{\mathrm{eff}}(\omega)|_{\epsilon^{-1}} = \frac{m}{\pi^2 e^2}\int_0^{\omega} \omega' \frac{n(\omega')}{[n^2(\omega')+\kappa^2(\omega')]^2}\kappa(\omega')\,d\omega' . \tag{8}$$

Comparison with Eq. (5) shows that from $\omega = 0$ to the point ω_1, where $n(\omega)$ first passes through unity

$$n_{\mathrm{eff}}(\omega)|_{\epsilon} > n_{\mathrm{eff}}(\omega)|_{\kappa} > n_{\mathrm{eff}}(\omega)|_{\epsilon^{-1}}, \quad 0 < \omega < \omega_1 , \tag{9}$$

since $n(\omega) > 1$ in this range. Moreover, from ω_h, the highest finite value of ω for which $n(\omega)$ is unity, to infinity $n(\omega) < 1$ so that the same equality must hold, since

$$n_{\mathrm{eff}}(\infty)|_{\epsilon} = n_{\mathrm{eff}}(\infty)|_{\kappa} = n_{\mathrm{eff}}(\infty)|_{\epsilon^{-1}} = N \tag{10}$$

and

$$\frac{d(n_{\mathrm{eff}}|_{\epsilon})}{d\omega} < \frac{d(n_{\mathrm{eff}}|_{\kappa})}{d\omega} < \frac{d(n_{\mathrm{eff}}|_{\epsilon^{-1}})}{d\omega}, \quad \omega_h < \omega < \infty . \tag{11}$$

In a simple system such as a Drude metal[6] or the single Lorentz oscillator model of an insulator[6] $n(\omega)$ crosses unity at only one finite value of ω. Consequently in these systems $\omega_1 = \omega_h$ and the ordering of Eq. (9) holds for all ω as is evident in Figs. 1(a) and 2(a). In more complex systems in which there can be multiple crossings of unity by $n(\omega)$ there does not appear to be a simple argument to establish the ordering of the values of $n_{\mathrm{eff}}(\omega)$ for $\omega_1 > \omega > \omega_h$. However, recent studies of aluminum and silicon by Shiles and Smith[8,9] and polystyrene by Inagaki *et al.*[10] suggest that the ordering of Eq. (9) is often maintained in real materials.

III. FINITE-ENERGY f SUMS

In general the three forms of $n_{\rm eff}(\omega)$ bear no simple relation to one another. However, in the idealized case in which the absorptions of a material may be divided into widely separated groups such as valence-electron and core-electron absorptions, a useful relation obtains. At energies less than those for core excitations the valence or conduction electrons of such a system may be regarded as moving in a transparent medium consisting of the ion cores with a real dielectric function $\epsilon_b(\omega)$. Then for energy $\hat{\omega}$ large compared with the absorption of the valence electrons, but below those for core excitations, the dielectric function is real and may be expanded[6]

$$\lim_{\omega\to\hat{\omega}} \epsilon(\omega)=\epsilon_b(\omega)-\omega^2_{p,v}/\omega^2+\cdots, \tag{12}$$

where $\omega_{p,v}$ is the plasma frequency of the valence or conduction electrons. In the limit of core excitations lying at frequencies very high compared with those for valence electrons, $\epsilon_b(\omega)$ may be taken as a constant, ϵ_b, and the limits of the optical constants are

$$\lim_{\omega\to\hat{\omega}} \epsilon(\omega)=\epsilon_b-\omega^2_{p,v}/\omega^2+\cdots, \tag{13}$$

$$\lim_{\omega\to\hat{\omega}} n(\omega)=\epsilon_b^{1/2}-\frac{\omega^2_{p,v}}{2\epsilon_b^{1/2}\omega^2}+\cdots, \tag{14}$$

and

$$\lim_{\omega\to\hat{\omega}} \epsilon^{-1}(\omega)=\epsilon_b^{-1}+\omega^2_{p,v}/\epsilon_b^2\omega^2+\cdots. \tag{15}$$

Finite f-sum rules may then be derived using standard methods employing a Cauchy-theorem integration about a semicircular path of radius $\hat{\omega}$ in the upper half plane.[11] The results are

$$\int_0^{\hat{\omega}} \omega'\epsilon_2(\omega')\,d\omega'\approx\frac{\pi}{2}\omega^2_{p,v}, \tag{16}$$

$$\int_0^{\hat{\omega}} \omega'\kappa(\omega')\,d\omega'\approx\frac{\pi}{4}\frac{\omega^2_{p,v}}{\epsilon_b^{1/2}}, \tag{17}$$

and

$$\int_0^{\hat{\omega}} \omega'\,\mathrm{Im}\left(\frac{1}{\epsilon(\omega')}\right)d\omega'\approx-\frac{\pi}{2}\frac{\omega^2_{p,v}}{\epsilon_b^2}. \tag{18}$$

These are exact in the limit of $\hat{\omega}\to\infty$ (this may be shown using superconvergence methods[4] with ω_b a constant at all frequencies). For finite $\hat{\omega}$ they are accurate[12] to within terms of the order of $\omega^2_{p,v}(\gamma/\hat{\omega})$, where γ is a damping constant equal to the width at half maximum of the valence-electron plasmon resonance in $\mathrm{Im}[\epsilon^{-1}(\omega)]$.

Comparing these three finite-energy rules with the definitions of $n_{\rm eff}(\omega)$ yields

$$n_{\rm eff}(\hat{\omega})|_\kappa=n_{\rm eff}(\hat{\omega})|_\epsilon/\epsilon_b^{1/2} \tag{19}$$

and

$$n_{\rm eff}(\hat{\omega})|_{\epsilon^{-1}}=n_{\rm eff}(\hat{\omega})|_\epsilon/\epsilon_b^2. \tag{20}$$

That is,

$$n_{\rm eff}(\hat{\omega})|_\epsilon : n_{\rm eff}(\hat{\omega})|_\kappa : n_{\rm eff}(\hat{\omega})|_{\epsilon^{-1}} :: 1 : \epsilon_b^{-1/2} : \epsilon_b^{-2}. \tag{21}$$

Note that these ratios are in accord with the inequalities of Eq. (9) even though $n(\omega)$ could cross unity at many points below $\hat{\omega}$.

The convergence of the finite-energy sum rules is illustrated in Figs. 1(b) and 2(b) for the same Lorentz insulator and Drude metal as in Figs. 1(a) and 2(a), but now assuming them embedded in a medium with a typical background dielectric constant $\epsilon_b=1.05$. The three functions have the same general shapes as the $\epsilon_b=1$ curves of Figs. 1(a) and 2(a); that is, they all rise monotonically from $\omega=0$ reaching gradually rising plateaus beyond the plasma frequency as the oscillator strength of the embedded valence electrons is exhausted. However, in the present case the plateaus do not coincide, but have heights in the ratios of $1:\epsilon_b^{-1/2}:\epsilon_b^{-2}$.

In this high-frequency limit the density of valence electrons

$$N_v=(m/4\pi e^2)\omega^2_{p,v} \tag{22}$$

is directly given by $n_{\rm eff}(\hat{\omega})|_\epsilon$ regardless of ϵ_b, whereas $n_{\rm eff}(\hat{\omega})|_\kappa$ and $n_{\rm eff}(\hat{\omega})|_{\epsilon^{-1}}$ depend on ϵ_b. Thus, it is consistent to identify $n_{\rm eff}(\hat{\omega})|_\epsilon$ as the number of electrons effective in real processes up to energy ω. On the other hand, $n_{\rm eff}(\hat{\omega})|_\kappa$ and $n_{\rm eff}(\hat{\omega})|_{\epsilon^{-1}}$ both involve ϵ_b and measure not only real processes below $\hat{\omega}$, but also virtual core-state processes above $\hat{\omega}$.

This point has practical consequences in the analysis of electron energy-loss experiments where $\mathrm{Im}(\epsilon^{-1})$ is often incorrectly normalized by applying the f-sum rule in the form of Eq. (18), but without accounting for the ϵ_b^2 factor in the denominator.

IV. EFFECTS OF FINITE $\hat{\omega}$ AND DISPERSION IN $\epsilon_b(\omega)$

The results of Sec. III allow the determination of ϵ_b from the valence-electron spectrum provided $\hat{\omega}$ is taken to a sufficiently high frequency that the oscillator strength of the valence electrons is exhausted. In practice, oscillator-strength exhaustion is only approximately achieved before an x-ray edge is encountered. Moreover, at higher energies dispersion in the background dielectric function $\epsilon_b(\omega)$ may become significant, invalidating the approximation of a constant ϵ_b made in Eq. (12). It is therefore of interest to consider how ϵ_b as determined from values of $n_{\rm eff}(\omega)$ differs from the actual ϵ_b for f sums taken to a frequency $\hat{\omega}$ that is only a small multiple of $\omega_{p,v}$.

The values of ϵ_b calculated from Eqs. (19) and (20) using values of $n_{\rm eff}(\hat{\omega})$ from the model calcu-

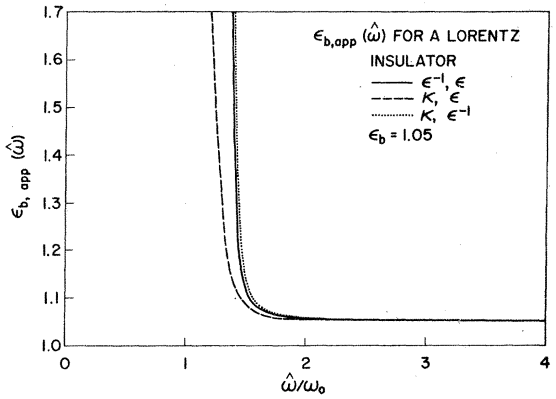

FIG. 3. Apparent values of the background dielectric constant calculated from Eqs. (19), (20), and (23) as a function of the upper limit of the finite f sums for a model insulator. Values of $n_{\text{eff}}(\omega)$ shown in Fig. 1(b) for the single Lorentz oscillator model with $\epsilon_b = 1.05$ were employed. The curve labeled κ, ϵ was calculated via Eq. (19) from $n_{\text{eff}}(\hat{\omega})|_\kappa$ and $n_{\text{eff}}(\hat{\omega})|_\epsilon$, similarly ϵ^{-1}, ϵ denotes the calculation based on Eq. (20) and κ, ϵ^{-1} the calculation using Eq. (23). At $\hat{\omega} = 3\omega_0$ $\epsilon_{b,\text{app}}(\hat{\omega})$ differs from ϵ_b by less than 0.001 for all calculations.

lations of Figs. 1(b) and 2(b) for $\epsilon_b = 1.05$ are given in Figs. 3 and 4 as a function of $\hat{\omega}$. These apparent values are denoted by $\epsilon_{b,\text{app}}(\hat{\omega})$. Curves labeled κ, ϵ (dashed curve) and ϵ^{-1}, ϵ (solid curve) are the values for $[n_{\text{eff}}(\omega)|_\epsilon / n_{\text{eff}}(\omega)|_\kappa]^2$ and $[n_{\text{eff}}(\omega)|_\epsilon / n_{\text{eff}}(\omega)|_{\epsilon^{-1}}]^{1/2}$, respectively. In the case of the Drude metal (Fig. 4) sets of curves for two different values of the parameter[6] ω_p/γ are given. The value $\omega_p/\gamma \approx 20$ is representative of metallic aluminum

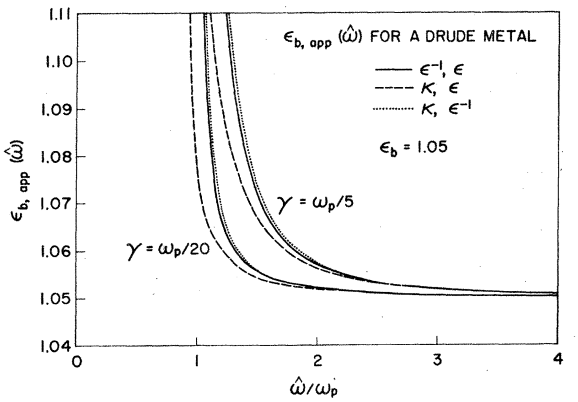

FIG. 4. Apparent values of the background dielectric constant calculated from Eqs. (19), (20), and (23) as a function of the upper limit of the finite f sums for a model metal. Values of $n_{\text{eff}}(\omega)$ for the Drude metal with $\epsilon_b = 1.05$, similar to those shown in Fig. 2(b) were used; the only change was to use γ values of $\frac{1}{20}\omega_p$ and $\frac{1}{5}\omega_p$ rather than $\frac{1}{10}\omega_p$. The $\gamma = \frac{1}{10}\omega_p$ values pass between the curves shown.

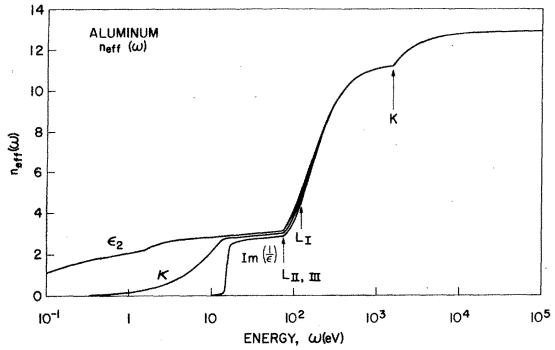

FIG. 5. Values of $n_{\text{eff}}(\hat{\omega})$ for metallic aluminum after Shiles and Smith, Ref. 7. Position of the three L edges and the K edge are shown by arrows. Note that $n_{\text{eff}}(\omega)|_\epsilon$ exceeds 3 below the L edge because of redistribution of oscillator strength from the core electrons. The core-electron oscillator strength is reduced by a corresponding amount so that the f sum rule is satisfied by the atom as a whole.

near the plasma frequency.

In general the calculated values of $\epsilon_b(\hat{\omega})$ are greater than the actual background value. However, at frequencies greater than $2\omega_{p,v}$ the calculated values approach the actual value rather closely, and for representative values of the electron damping, $\epsilon_{b,\text{app}}(\omega) - 1$ is within better than 5% of $\epsilon_b - 1$ by $\hat{\omega} = 3\omega_{p,v}$. Thus it appears that values of ϵ_b can be reliably estimated from $n_{\text{eff}}(\hat{\omega})$ provided the upper limit of the f sum is chosen to be several times the valence-electron plasma frequency, i.e., for frequencies at which values of $n_{\text{eff}}(\omega)$ have reached the slowly rising but parallel plateaus.

An alternative means of calculating ϵ_b is to eliminate $n_{\text{eff}}(\omega)|_\epsilon$ from Eqs. (19) and (20) to obtain

$$\epsilon_b = [n_{\text{eff}}(\hat{\omega})|_\kappa / n_{\text{eff}}(\hat{\omega})|_{\epsilon^{-1}}]^{2/3}. \tag{23}$$

In practice, this form is more useful than Eqs. (19) and (20) in the case of metals where optical data in the far infrared is unreliable or lacking. The reason is that the infrared portion of the spectrum makes a larger contribution to $n_{\text{eff}}(\omega)|_\epsilon$ than to either $n_{\text{eff}}(\omega)|_\kappa$ or $n_{\text{eff}}(\omega)|_{\epsilon^{-1}}$ [see Figs. 2(a), 2(b), and 5]. Consequently, calculation of ϵ_b from Eq. (23) is less sensitive to uncertainties in the infrared. The dependence of $\epsilon_{b,\text{app}}(\hat{\omega})$ on $\hat{\omega}$ as calculated from Eq. (23) is similar to that for values calculated from $n_{\text{eff}}(\hat{\omega})|_\epsilon$ and $n_{\text{eff}}(\hat{\omega})|_{\epsilon^{-1}}$ via Eq. (20). This is shown for the model examples by the dotted curve labeled κ, ϵ^{-1} in Figs. 3 and 4.

The qualitative effects of dispersion may be seen by a similar model calculation in which the apparent values of the background $\epsilon_{b,\text{app}}(\hat{\omega})$ is calculated from optical constants modeled with a dispersive $\epsilon_b(\omega)$. Qualitatively the result of such a calculation

is that for dispersions of the magnitude found in practice $\epsilon_{b,\mathrm{app}}(\hat{\omega})-1$ is a few percent greater than if dispersion is neglected. Further, $\epsilon_{b,\mathrm{app}}(\hat{\omega})$ calculated from $n_{\mathrm{eff}}|_K$ and $n_{\mathrm{eff}}|_\epsilon$ is always somewhat smaller than that calculated from $n_{\mathrm{eff}}|_{\epsilon^{-1}}$ and $n_{\mathrm{eff}}|_\epsilon$. The reason is that $\kappa(\omega)$ is appreciable at lower values of ω than $\mathrm{Im}[\epsilon^{-1}(\omega)]$ and consequently samples a somewhat smaller value of $\epsilon_b(\omega)$.

V. $n_{\mathrm{eff}}(\omega)$ FOR METALLIC ALUMINUM

As an example of the finite-energy f-sum rules values of $n_{\mathrm{eff}}(\omega)$ from the infrared to well beyond the K-shell excitation energy for metallic aluminum are shown in Fig. 5. The optical constants used are those suggested by Shiles and Smith's[8] analysis of currently available experimental data for aluminum (see Sec. VI). The gross features of these functions are representative of $n_{\mathrm{eff}}(\omega)$ for third-period elements: the optical properties in the infrared, visible, and ultraviolet are primarily determined by $3s$ and $3p$ valence-electron excitations; the L-shell excitations lie in the range from 30 to 250 eV and K-shell excitations occur between 1 and 3 keV.[13] The oscillator strength of the three valence electrons of the $3s^23p$ configuration in aluminum is almost exhausted above the valence-electron plasma frequency at approximately 15 eV. Above this the various values of $n_{\mathrm{eff}}(\omega)$ all level off forming three distinct but parallel plateaus, which rise slowly from 20 eV to the L edge at 72.65 eV. In this region the three values differ because of the shielding effects of $1s$, $2s$, and $2p$ ion core levels. Just below the L edge, $n_{\mathrm{eff}}(\omega)|_\epsilon$ saturates at approximately 3.2 e/at. As discussed above, this corresponds to the conventional oscillator strength. The fact that the valence-electron strength exceeds 3 by some 7% is a consequence of the Pauli principle redistribution[6,14] of oscillator strength from core transitions which are weakened by a corresponding amount. Above the $L_{\mathrm{II,III}}$ edge the values of $n_{\mathrm{eff}}(\omega)$ rise abruptly as the eight L electrons contribute to direct optical processes. The values of $n_{\mathrm{eff}}(\omega)$ draw together and by several hundred eV they are indistinguishable to within computational accuracy. In this range the polarizable background is that of the $1s$ core levels only, and from the L edge to well beyond 700 eV the background dielectric function exceeds unity by less than 10^{-4}. The f sums again reach a plateau as the L-shell oscillator strength is exhausted only to rise again at the K edge and saturate at 13 e/at. in the high-frequency limit.

Over the range from 30 to 72.65 eV the ratios of $n_{\mathrm{eff}}(\omega)|_\epsilon$, $n_{\mathrm{eff}}(\omega)|_K$, and $n_{\mathrm{eff}}(\omega)|_{\epsilon^{-1}}$ are constant to within the accuracy of the calculation. Since there are no data in the very far infrared, ϵ_b is best evaluated with Eq. (23). The results range from 1.04_4 at 30 eV to 1.03_5 at 72.5 eV.

An independent estimate of $\epsilon_b(\omega)$ may be made from a Kramers-Kronig transformation of $\epsilon_2(\omega)$ omitting all absorption below the L edge. This yields a static dielectric constant of 1.03. There is a small dispersion in $\epsilon_b(\omega)$, but it remains approximately 1.03 up to 35 eV rising to 1.04 at 50 eV. The agreement between this and the values given by Eq. (23) is well within the accuracy of the calculation and is in accord with the model proposed in Sec. III.

VI. SELF-CONSISTENCY TESTS

The finite f-sum rules for the valence electrons provide a useful test of the optical constants below the onset of core excitations. As such they may be employed to check the self-consistency of composite data and Kramers-Kronig transforms. The graph of n_{eff} in Fig. 5 employs optical constants for aluminum, which were derived by a self-consistent analysis of a variety of optical data, in which particular care was taken to treat the infrared and x-ray regions as accurately as available data would allow. However, the literature abounds in data for which the infrared and x-ray spectra are neglected or inadequately treated, and in cases for which the various valence oscillator-strength sums are constrained to saturate to the number of valence electrons.

From the considerations of this paper it is clear that neglect of the x-ray spectra leads to equality of all values of $n_{\mathrm{eff}}(\omega)$ in the high-energy limit, but on the average causes errors of the order of ϵ_b-1, $\frac{1}{2}(\epsilon_b-1)$, and $2(\epsilon_b-1)$ in $\epsilon(\omega)$, $\tilde{n}(\omega)$, and $\epsilon^{-1}(\omega)$, respectively. In our example of aluminum this can amount to 8% to 10% errors for $\epsilon^{-1}(\omega)$.

The relative importance of the infrared region of the spectrum to the various f sums for a metal can be seen from Figs. 2(a), 2(b), and 5. For aluminum, $n_{\mathrm{eff}}(\omega)|_\epsilon$ receives a major contribution from below 0.1 eV, while $n_{\mathrm{eff}}(\omega)|_K$ and $n_{\mathrm{eff}}(\omega)|_{\epsilon^{-1}}$ are insensitive to the optical properties there. Consequently, errors in the infrared region will be reflected primarily in $n_{\mathrm{eff}}(\omega)|_\epsilon$. In particular, neglect or underestimation of the infrared absorption causes $n_{\mathrm{eff}}(\omega)|_\epsilon$ to be too small and to fall below $n_{\mathrm{eff}}(\omega)|_K$ and $n_{\mathrm{eff}}(\omega)|_{\epsilon^{-1}}$ at high frequencies. This is a common feature of a number of published compilations[15] and suggests incorrect or inadequate extrapolation in the infrared.

ACKNOWLEDGMENTS

The authors would like to thank Dr. M. Inokuti and Dr. T. Sasaki for discussions on the self-consistent

analysis of optical data and Professor D. L. Dexter for helpful comments on an early version of the manuscript. This work is based on research performed under the auspices of the U.S. Department of Energy.

[1]H. A. Bethe and E. E. Salpeter, *Quantum Mechanics of One- and Two-Electron Atoms* (Springer-Verlag, Berlin, 1957).

[2]See, for example, H. Ehrenreich, in *The Optical Properties of Solids*, edited by J. Tauc (Academic, New York, 1966), Sec. 9, p. 106.

[3]M. Altarelli, D. L. Dexter, H. M. Nussenzveig, and D. Y. Smith, Phys. Rev. B 6, 4502 (1972).

[4]For a similar model applied to the optical constants of the alkali metals, see M. H. Cohen, Philos. Mag. 3, 762 (1958).

[5]M. Altarelli and D. Y. Smith, Phys. Rev. B 9, 1290 (1974).

[6]See, for example, F. Wooten, *Optical Properties of Solids* (Academic, New York, 1972).

[7]The parameters for the optical-constant models are defined by the Lorentz formula

$$\epsilon_1(\omega) + i\,\epsilon_2(\omega) = \epsilon_b - \omega_p^2/(\omega^2 - \omega_0^2 + i\,\gamma\omega).$$

[8]E. Shiles and D. Y. Smith, Bull. Am. Phys. Soc. 22, 92 (1977); and unpublished.

[9]E. Shiles and D. Y. Smith, Bull. Am. Phys. Soc. 23, 226 (1978); and unpublished.

[10]T. Inagaki, E. T. Arakawa, R. N. Hamm, and M. W. Williams, Phys. Rev. B 15, 3243 (1977).

[11]See, for example, C. Ferro Fontan, N. M. Queen, and G. Violini, Riv. Nuovo Cimento 2, 357 (1972).

[12]Corrections to Eqs. (16)–(18) for finite $\hat{\omega}$ may be estimated as the integral from $\hat{\omega}$ to ∞ for the asymptotic form of the appropriate Drude or Lorentz model. The Drude model yields

$$\int_{\hat{\omega}}^{\infty} \omega' \epsilon_2(\omega')\, d\omega' = \omega_p^2 \left(\frac{\pi}{2} - \tan^{-1}\frac{\hat{\omega}}{\gamma}\right).$$

An equivalent procedure is to calculate the integral of the higher-order terms of Eqs. (13)–(15) along the semicircular path of radius $\hat{\omega}$ in the upper half of the complex plane. In the case of aluminum, discussed in Sec. V, corrections for cutting off the f sums at the L edge (72.65 eV) are of the order of 0.02 e/at. out of total f sums of some 3 e/at., i.e., less than a 1% correction.

[13]G. L. Clark, in *Handbook of X-Rays*, edited by E. F. Kaelble (McGraw-Hill, New York, 1967).

[14]See, for example, D. Y. Smith and D. L. Dexter, in *Progress in Optics*, edited by E. Wolf (North-Holland, Amsterdam, 1972), Vol. X, Sec. 3.2; and Ref. 5, p. 77.

[15]For a review with several examples see, C. Kunz, in *Optical Properties of Solids—New Developments*, edited by B. O. Seraphin (North-Holland, Amsterdam, 1976), Chap. 10, Table 2.